

## Notable difference in anti-HIV activity of integrase inhibitors as a consequence of geometric and enantiomeric configurations

Maurice Okello, Sanjay Mishra, Malik Nishonov, Vasu Nair\*

UGA Center for Drug Discovery, the College of Pharmacy, R.C. Wilson Pharmacy Bldg., Room 320, University of Georgia, Athens, GA 30602, USA

### ARTICLE INFO

#### Article history:

Received 9 April 2013

Revised 10 May 2013

Accepted 13 May 2013

Available online 23 May 2013

#### Keywords:

Integrase

Anti-HIV

Enantiomers

Drug discovery

Cytochrome P450 isozymes

### ABSTRACT

While some examples are known of integrase inhibitors that exhibit potent anti-HIV activity, there are very few cases reported of integrase inhibitors that show significant differences in anti-HIV activity that result from distinctions in *cis*- and *trans*-configurations as well as enantiomeric stereostructure. We describe here the design and synthesis of two enantiomeric *trans*-hydroxycyclopentyl carboxamides which exhibit notable difference in anti-HIV activity. This difference is explained through their binding interactions within the active site of the HIV-1 integrase intasome. The more active enantiomer **3** (EC<sub>50</sub> 25 nM) was relatively stable in human liver microsomes. Kinetic data revealed that its impact on key cytochrome P450 isozymes, as either an inhibitor or an activator, was minor, suggesting a favorable CYP profile.

© 2013 Elsevier Ltd. All rights reserved.

HIV-1 integrase is a 32 kDa protein, which catalyzes the incorporation of HIV DNA into host chromosomal DNA through a specifically defined sequence of reactions, which involves 3'-processing and a key strand transfer (ST) step.<sup>1–6</sup> Initiation of integration occurs in the cytoplasm, where a complex is formed between viral cDNA, previously produced by reverse transcription, and HIV integrase. Following this is site-specific endonucleatic cleavage of two nucleotides from each 3'-end of double-stranded viral DNA, which produces truncated viral DNA with terminal CAOH-3' (3'-processing). The next step, ST, involves staggered nicking of chromosomal DNA and joining of each 3'-end of the recessed viral DNA to the 5'-ends of the host DNA, followed by repair/ligation. The ST step is carried out after transport of the processed, preintegration complex from the cytoplasm into the nucleus. Both 3'-processing and ST steps require divalent metal ions as cofactors.

We recently reported on the synthesis and structure-activity studies of new anti-HIV-1 integrase inhibitors.<sup>7</sup> Among the most interesting compounds discovered in this study was 4-(5-(2,4-difluorobenzyl)-1-(2-fluorobenzyl)-2-oxo-1,2-dihydropyridin-3-yl)-4-hydroxy-2-oxobut-3-enoic acid (**1**, Fig. 1), which exhibited potent strand transfer (ST) inhibitory activity (IC<sub>50</sub> 6 nM). However, the in vitro antiviral data of compound **1** revealed that there was a significant disconnect of almost two orders of magnitude between the anti-HIV-1 activity in cell culture (EC<sub>50</sub> 500 nM, MAGI cells) and the low nM ST IC<sub>50</sub> data for **1**. Because this disconnect appeared to be a problem associated with the cellular permeability of this ionized

inhibitor, we investigated unionized and somewhat more lipophilic derivatives of inhibitor **1**. Interesting new compounds to emerge from this study were the hydroxycyclopentyl carboxamides **2** (Fig. 2, clogP 3.41). However, while the racemic *trans*-compound showed strong strand transfer inhibition of HIV-1 integrase with an IC<sub>50</sub> of 48 nM, the racemic *cis*-compound was not an inhibitor of integrase.<sup>8</sup>

To explore further whether enantiomers belonging to the *trans*-compound related to **2** would show significant differences in anti-HIV activity in cell culture as a consequence of their specific chirality, we synthesized their optically pure (*S,S*) and (*RR*) enantiomeric hydroxycarboxamides, **3** and **4** (Fig. 2).

Synthesis of the enantiomeric carboxamides was achieved from **1**, which was prepared from 5-bromo-2-methoxypyridine **5** via the acetylpyridinone **7**,<sup>7</sup> as summarized in Scheme 1. Conversion of diketo acid **1** to produce the optically active carboxamide **3** required the coupling amine, (1*S*,2*S*)-(+)-*trans*-2-aminocyclopentanol (Sigma–Aldrich). Treatment of **1** in DMF with hydroxybenzotriazole (HOBt) followed by 1-(3-dimethylaminopropyl)-3-ethylcarbodiimide hydrochloride (EDCI–HCl) produced the activated intermediate of **1**, which was coupled using (1*S*,2*S*)-(+)-*trans*-2-aminocyclopentanol hydrochloride in the presence of NaHCO<sub>3</sub>. Purification of the resulting crude product using silica gel chromatography gave highly purified (1*S*,2*S*)-4-(5-(2,4-difluorobenzyl)-1-(2-fluorobenzyl)-2-oxo-1,2-dihydropyridin-3-yl)-4-hydroxy-*N*-(2-hydroxycyclopentyl)but-3-enamide (**3**) in 66% yield ([α]<sub>D</sub><sup>20</sup> +41.8, c 0.01, CH<sub>3</sub>OH).<sup>9</sup> The enantiomer of **3**, that is, compound **4**, was prepared by a similar route, but using (1*R*,2*R*)-2-aminocyclopentanol hydrochloride as the coupling reagent.<sup>10</sup> This coupling reagent was

\* Corresponding author. Tel.: +1 (706) 542 6293; fax: +1 (706) 583 8283.

E-mail address: [vnair@rx.uga.edu](mailto:vnair@rx.uga.edu) (V. Nair).

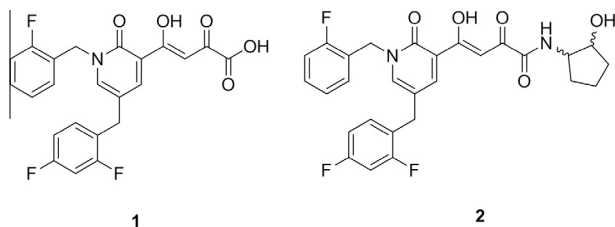


**Figure 1.** Structures of HIV-1 integrase inhibitor **1** and four possible hydroxycyclopentyl carboxamides **2**.

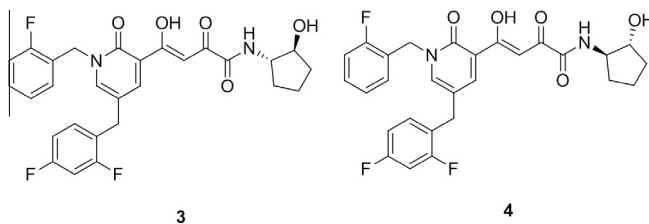


**Figure 2.** Structures of the (*S,S*) and (*R,R*) enantiomers (**3** and **4**) of the *trans*-isomer of compound **2**.

synthesized using a modification of a literature procedure.<sup>11</sup> The yield of pure compound **4** from **1** was 42% ( $[\alpha]_D^{20}$  –41.2, *c* 0.01, CH<sub>3</sub>OH).

A summary of the in vitro anti-HIV-1 NL4-3 data of **3** and **4** in MAGI cells are shown in Table 1.<sup>8</sup> With respect to the EC<sub>50</sub> data, it is evident that both compounds are active and show low nM cell culture activity. However, the data also clearly indicate that the (*S,S*)-isomer **3** was more active than its (*R,R*)-enantiomer **4**, in terms of both the EC<sub>50</sub> and EC<sub>90</sub> anti-HIV data. The question then was to see if this difference in viral replication inhibition could be explained through the molecular details of the interaction of these compounds with the HIV-1 intasome (i.e., HIV-1 integrase-processed viral DNA complex) and this is discussed below.

Comparison of the binding interactions of compounds **3** and **4** within the modeled active site of HIV-1 integrase intasome was carried out through docking experiments in order to provide an explanation for the difference in antiviral activity.<sup>12</sup> The results are shown in Figure 3. The amino acid residues are designated with HIV-1 numbering and are color coded by hydrophobicity with the orange color indicating more hydrophobicity and the blue color indicating less hydrophobicity. Atoms of DNA residues and of inhibitors **3** and **4** (ball and stick representation) are colored according to atom type: carbon—grey; nitrogen—blue; oxygen—red; fluorine—

**Table 1**

In vitro anti-HIV-1 data of compounds **3** and **4** in MAGI cells

Inhibitor	EC <sub>50</sub> (SD) nM	EC <sub>90</sub> (SD) nM	CC <sub>50</sub> (μM)
<b>3</b> ( <i>S,S</i> -Enantiomer)	25.1 (±3.9)	415.1 (±39.1)	40.4 (±1.9)
<b>4</b> ( <i>R,R</i> -Enantiomer)	42.2 (±1.3)	871.4 (±23.5)	137.0 (±6.0)

EC<sub>50</sub> = concentration for 50% inhibition of virus replication. Mean of three determinations.

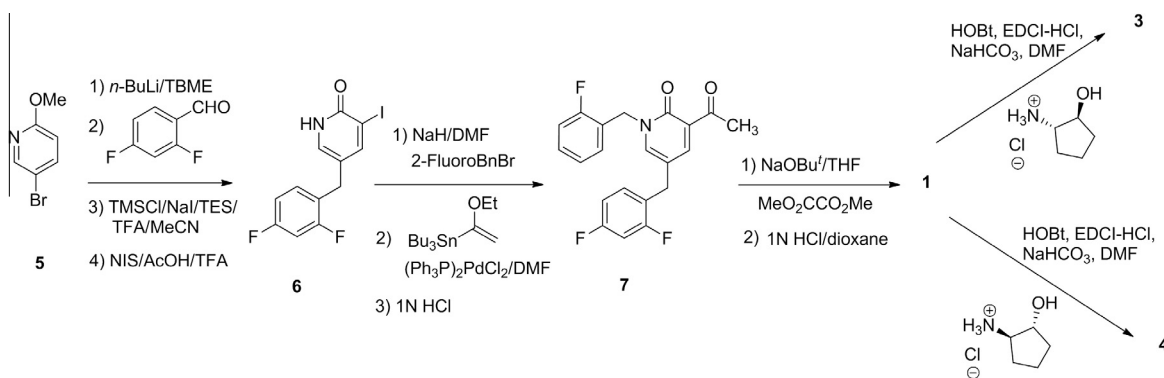
EC<sub>90</sub> = concentration for 90% reduction of virus replication. Mean of three determinations.

CC<sub>50</sub> = concentration to reduce cell viability by 50%.

green; hydroxyl hydrogen—cyan. Notable interactions common to both compounds include: non-polar interactions involving Pro145; polar interactions with two Mg<sup>2+</sup> ions, that is, chelation with diketo chromophore in both compounds; pi–pi stacking interaction of DC16 with the *o*-fluorophenyl ring and pi stacking of DA17 with the diketo chromophore. However, molecular modeling images in Figure 3C and D (partial structures shown) clearly show the difference in spatial orientation of the cyclopentyl carboxamide moiety of compounds **3** and **4** within the HIV-1 integrase intasome active site. This difference is in the interactions involving amino acid residues 143 and 118 within the active site. Compound **3** interacts with Tyr143 through the cyclopentylhydroxyl hydrogen and the aromatic pi-electrons of Tyr143. This interacting distance is about 2.8 Å.<sup>14</sup> The corresponding interaction is absent in the case of enantiomer **4**, which apparently forms a hydrogen bond with Gly118 in which the amide carbonyl oxygen of Gly118 is the acceptor.<sup>15,16</sup> The tyrosine ring is significantly further away (>6.0 Å) from the cyclopentyl OH in **4** to allow for the hydroxyl hydrogen–pi interaction seen in **3**. Our docking studies also indicated that the protein–ligand binding free energy favored compound **3**.

Because of the importance of establishing early, the behavior of a potentially promising new anti-HIV compound in phase I metabolism, our next studies involved the more active compound **3** and its in vitro microsome stability as well as its cytochrome P450 (CYP) profile.<sup>17–19</sup> The microsome stability studies were performed through incubations using pooled, mixed-gender human liver microsomes.<sup>20</sup> Analyses were performed by HPLC separation combined with UV detection and further bioanalytical identification of compound **3** and its metabolites. The results showed that compound **3** was relatively stable in pooled human liver microsomes (Fig. 4), exhibiting a half-life (*t*<sub>1/2</sub>) of approximately 2 h.

The CYP isozyme profile study also utilized pooled mixed-gender human liver microsomes and two substrates for CYP 3A4 (testosterone and triazolam) and one substrate for CYP 2D6 (dextromethorphan).<sup>21</sup> These two CYP isozymes account for the metabolism of about 80% of the drugs that are metabolized in



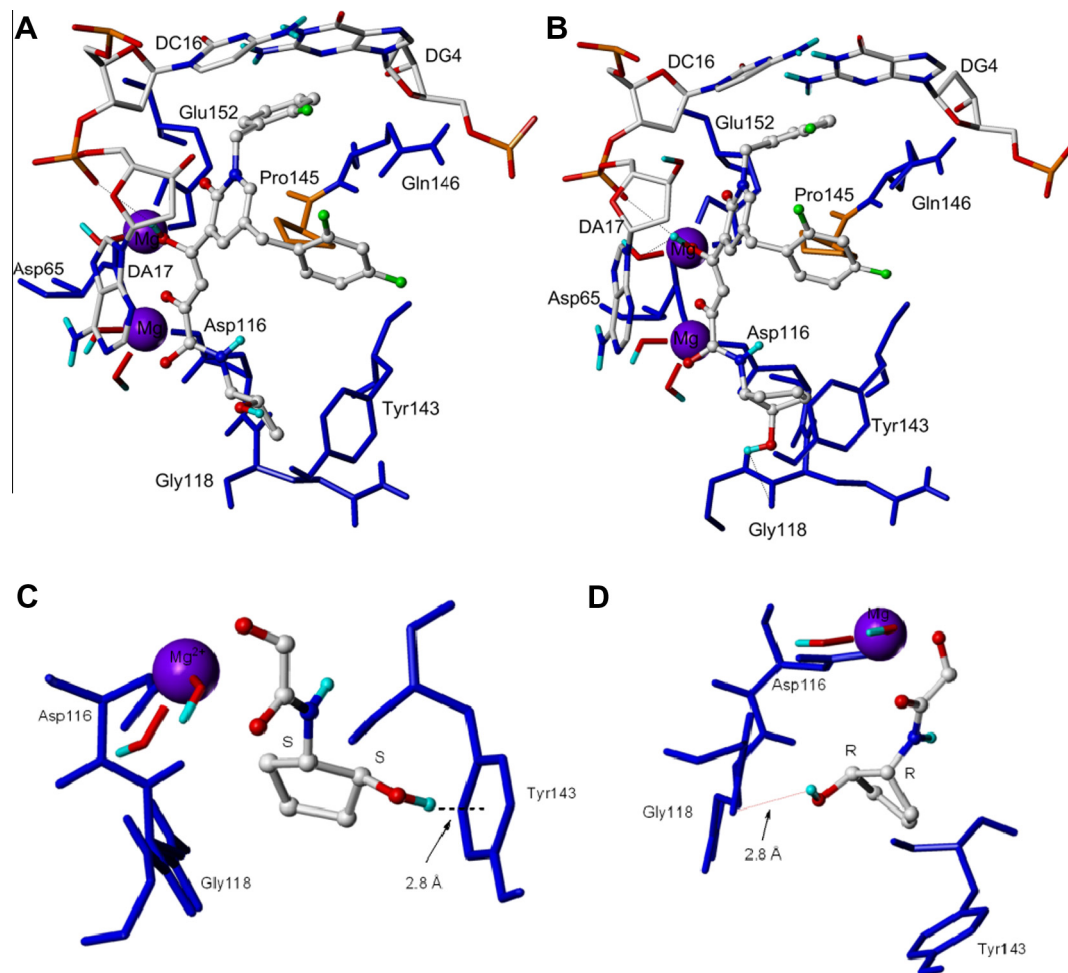


**Figure 3.** Docking of HIV integrase inhibitor **3**: A and C and **4**: B and D with the integrase catalytic site of the HIV-1 integrase–DNA intasome (PDB code 3OAY).<sup>13</sup> DNA residues and inhibitor atom types: carbon—grey, nitrogen—blue, oxygen—red, fluorine—green, hydroxyl hydrogen—cyan. *R* and *S* are stereocenter designations.

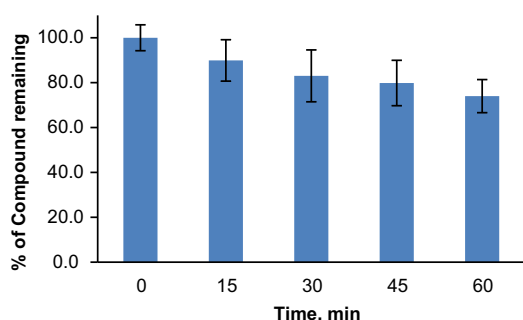


**Figure 4.** Stability of compound **3** in pooled, mixed-gender human liver microsomes. Data bars indicate the mean from three determinations. The error bars are standard deviations ( $\pm$ S.D.s) from the mean.

phase I metabolism by CYP isozymes.<sup>17</sup> Summarized in Table 2 is the effect of compound **3** on the substrate activity of these key CYP isozymes (CYP3A4—hydroxylation of testosterone and triazolam, and CYP2D6—demethylation of dextromethorphan). The data indicate only relatively small changes in the level of substrate activity compared to the control study in each case. Changes in compound **3** concentration also did not influence significantly the inhibition or activation of the probe substrates. The data ob-

served were generally within expected experimental variations. Thus, compound **3** is neither a significant inhibitor nor an activator of these key CYP isozymes and its CYP profile appears to be favorable with respect to these key isozymes.

In summary, there are very few examples known of integrase inhibitors that show significant differences in anti-HIV activity that result from distinctions in *cis*- and *trans*-configurations as well as enantiomeric stereostructure. We have described herein the stereospecific synthesis of two enantiomeric *trans*-hydroxycyclopentyl carboxamides. The (*S,S*)-enantiomer **3** was notably more active than its (*R,R*)-counterpart **4** on the basis of both the EC<sub>50</sub> and EC<sub>90</sub> data in anti-HIV-1 assays in cell culture. This difference in antiviral activity may be explained by examining the molecular level interactions of these compounds with the HIV-1 integrase intasome. The more active (*S,S*)-compound, on which further study was continued, was moderately stable in pooled, mixed-gender human liver microsomes. Kinetic data showed that its behavior towards key cytochrome P450 isozymes, either as an inhibitor or an activator, was relatively minor, suggesting that the compound is expected to possess a generally favorable CYP profile. Further studies are in progress on the molecular design and synthesis, antiviral evaluations and CYP studies of novel integrase-based anti-HIV compounds, in which preferred configurational geometry and enantiomeric structure are both critical for significant antiviral activity.

**Table 2**Influence of compound **3** on CYP isozyme substrate activity in pooled human liver microsomes

CYP isozyme	Substrate	Probe substrate concentration <sup>a</sup> (μM)	Compound <b>3</b> concentration (μM)	Substrate activity % ±S.D. <sup>b</sup>
CYP 3A4	Testosterone	100		Control
CYP 3A4	Testosterone	100	12.5	109 ± 13
CYP 3A4	Testosterone	100	25	97 ± 18
CYP 3A4	Testosterone	100	50	112 ± 15
CYP 3A4	Triazolam	200		Control
CYP 3A4	Triazolam	200	12.5	124 ± 23
CYP 3A4	Triazolam	200	25	98 ± 7
CYP 3A4	Triazolam	200	50	100 ± 8
CYP 2D6	Dextromethorphan	200		Control
CYP 2D6	Dextromethorphan	200	12.5	86 ± 7
CYP 2D6	Dextromethorphan	200	25	87 ± 17
CYP 2D6	Dextromethorphan	200	50	87 ± 13

<sup>a</sup> The concentration of each probe substrate was determined by the  $K_m$  value for that substrate.<sup>17</sup><sup>b</sup> Change in substrate activity (%) relative to the control value (100%). Standard deviations (±S.D.) were determined from the mean of three determinations. Substrate and metabolite peaks were monitored by HPLC–UV bioanalytical methods.<sup>21</sup>

## Acknowledgments

This project was supported by research Grant RO1 AI 43181 (NIAID) and shared equipment Grant IS10RR016621 (NCRR) from the National Institutes of Health. The contents of this submission are solely the responsibility of the authors and do not necessarily represent the official views of the NIH. We thank the Terry Endowment, the Georgia Research Alliance and the University of Georgia for additional support. Some of the data cited here were determined at Inhibitex, Inc., Alpharetta, GA and at the Southern Research Institute, Frederick, MD and we express our thanks to them.

## References and notes

- Frankel, A. D.; Young, J. A. T. *Annu. Rev. Biochem.* **1998**, *67*, 1.
- Asante-Appiah, E.; Skalka, A. M. *Adv. Virus Res.* **1999**, *52*, 351.
- Nair, V.; Chi, G. *Rev. Med. Virol.* **2007**, *17*, 277.
- Krishnan, L.; Engleman, A. J. *Biol. Chem.* **2012**, *287*, 40858.
- Nair, V.; Chi, G. In *HIV-1 Integrase: Mechanism and Inhibitor Design*; Neamati, N., Ed.; Wiley: Hoboken, New Jersey, 2011; pp 379–388.
- Liao, C.; Marchand, C.; Burke, T. R.; Pommier, Y.; Nicklaus, M. C. *Future Med. Chem.* **2010**, *2*, 1107.
- Seo, B. I.; Uchil, V. R.; Okello, M.; Mishra, S.; Ma, X.-H.; Nishonov, M.; Shu, Q.; Chi, G.; Nair, V. *ACS Med. Chem. Lett.* **2011**, *2*, 877.
- Integrase inhibition and antiviral assays. Integrase inhibition assay*: DNA substrate (final concentration 20 nM), serial dilutions of test compounds (starting from 1.5 μM) and HIV-1 integrase (final concentration 1 μg/well) (Bioproducts, MD) were combined in a reaction buffer (10 mM MgCl<sub>2</sub>, 20 mM HEPES (pH 7.5), 5% PEG, 0.1 mg/mL BSA, 5 mM DTT) at a final volume of 40 μL/well of a 96 well polypropylene plate. The mixture is incubated for 1 h at 37 °C. After the reaction was completed, the mixtures were adjusted to 20 mM Tris–Cl (pH 8.0), 400 mM NaCl, 10 mM EDTA + 0.1 mg/mL sonicated salmon sperm DNA at 100 μL/well final volume. The mixture was transferred to a 96 well Streptavidin coated ELISA plates (Nunc). The plates were incubated for 1 h at room temperature. Following the incubation, the plate was washed 3 times with 200 μL/well 30 mM NaOH, 200 mM NaCl, 1 mM EDTA followed by 3× with 200 μL/well 10 mM Tris–Cl (pH 8.0), 1 mM EDTA. The wash solutions were incubated on the plate for 5 min between each wash. The final product was detected using Sheep anti-Digoxigenin-POD, Fab fragments (1:200 dilution; 1 h incubation at 37 °C) (Roche). Unbound detection antibody was removed with 6 washes of 1× PBS, 0.1% Tween-20 (350 μL/wash using a plate washer). 100 μL of TMB substrate (KPL) was incubated on the plate for 10 min at room temperature followed by the addition of 100 μL/well of TMB stop solution (KPL). The absorbance values were read at 450 nm using the SpectraMax M2 Plate Reader from Molecular Devices. *Antiviral assay*. MAGI cells are infected with HIV-1 in the presence of test compound. If the virus is able to infect and replicate in the cells, it will proceed through reverse transcription and integration and begin transcription from the integrated provirus. One of the first virus proteins produced is HIV-1 Tat, which transactivates the HIV-1 LTR promoter, driving expression of β-galactosidase from an LTR-β-galactosidase reporter construct engineered into the cells. As a result, infected cells begin to overproduce the β-galactosidase enzyme. After 6 days post infection, the cells are lysed and β-galactosidase enzyme activity is measured using chemiluminescence detection (Perkin–Elmer Applied Biosystems). Compound toxicity is monitored on replicate plates using MTS dye reduction (CellTiter 96® Reagent, Promega, Madison, WI).
- Synthesis of (1*S*,2*S*)-4-(5-(2,4-difluorobenzyl)-1-(2-fluorobenzyl)-2-oxo-1,2-dihydropyridin-3-yl)-4-hydroxy-*N*-(2-hydroxycyclopentyl)but-3-enamide (**3**): To a chilled solution of 4-(5-(2,4-difluorobenzyl)-1-(2-fluorobenzyl)-2-oxo-1,2-dihydropyridin-3-yl)-4-hydroxy-2-oxobut-3-enoic acid (**1**) (150 mg, 0.338 mmol) in dimethylformamide (DMF) (2.0 mL), was added hydroxybenzotriazole (HOBt) (50 mg, 0.372 mmol), followed by 1-(3-dimethylaminopropyl)-3-ethylcarbodiimide hydrochloride (EDCI–HCl, 71 mg, 0.372 mmol) and the mixture was stirred for 30 min. A solution of (1*S*,2*S*)-(+)-trans-2-aminocyclopentanol hydrochloride and NaHCO<sub>3</sub> (31 mg, 0.372 mmol) was added followed by stirring for 2 h at 0–5 °C. Cold water was added to the reaction mixture, which was then extracted with ethyl acetate (2 × 20 mL). The combined organic phase was separated, washed with water twice, then once with 1 N HCl solution, and finally with saturated aqueous NaHCO<sub>3</sub> solution. Concentration in vacuo afforded the crude product which was passed through a short silica gel column with chloroform as the eluting solvent. The eluent containing the product was concentrated and the resulting residue was triturated with hexanes, which afforded the product as a yellow solid in 117 mg (66%), mp 61–63 °C,  $[\alpha]_D^{20} +41.8$  (c 0.01, methanol), UV  $\lambda_{max}$  396 nm ( $\epsilon$  14,455, methanol). <sup>1</sup>H NMR (CDCl<sub>3</sub>, 500 MHz):  $\delta$  15.33 (br s, 1H), 8.16 (d, 1H,  $J$  = 2.0 Hz), 8.08 (s, 1H), 7.61–6.85 (m, 9H), 5.22 (s, 2H), 4.11 (m, 1H), 3.94 (m, 1H), 3.78 (s, 1H), 2.23 (m, 1H), 2.10 (m, 1H), 1.88 (m, 1H), 1.78 (m, 2H), 1.59 (m, 1H). <sup>13</sup>C NMR (CDCl<sub>3</sub>, 125 MHz):  $\delta$  181.3, 180.6, 163.4, 163.3, 162.4, 162.1, 162.0, 161.4, 161.3, 160.4, 160.1, 160.0, 159.2, 145.5, 143.9, 142.3, 141.6, 132.4, 132.4, 132.3, 131.5, 131.4, 131.3, 131.3, 131.2, 130.7, 130.6, 125.0, 124.9, 124.8, 122.8, 122.7, 122.5, 122.2, 122.1, 122.1, 117.1, 115.9, 115.7, 115.6, 111.9, 111.9, 111.8, 111.7, 104.7, 104.5, 104.3, 98.3, 79.5, 79.3, 61.0, 60.6, 51.5, 47.7, 47.3, 32.9, 32.8, 32.7, 30.8, 30.7, 30.5, 21.7, 21.5. HRMS: calcd for C<sub>28</sub>H<sub>26</sub>F<sub>3</sub>N<sub>2</sub>O<sub>5</sub> (M+H), 527.1794; found 527.1799.
- Synthesis of (1*R*,2*R*)-4-(5-(2,4-difluorobenzyl)-1-(2-fluorobenzyl)-2-oxo-1,2-dihydropyridin-3-yl)-4-hydroxy-*N*-(2-hydroxycyclopentyl)but-3-enamide (**4**): Compound **4** was synthesized using the procedure described above for compound **3**. The coupling compound, (1*R*,2*R*)-2-aminocyclopentanol hydrochloride, was synthesized by modification of a literature procedure.<sup>10</sup> The crude product was purified on silica gel to give **4** as a yellow solid (42%), mp 55–57 °C,  $[\alpha]_D^{20} -41.2$  (c 0.1, methanol), UV  $\lambda_{max}$  396 nm ( $\epsilon$  14,100, methanol). <sup>1</sup>H NMR (CDCl<sub>3</sub>, 500 MHz):  $\delta$  15.41 (br s, 1H), 8.16 (s, 1H), 8.07 (s, 1H), 7.60–6.84 (m, 9H), 5.21 (s, 2H), 4.10–3.76 (m, 5H), 2.25–1.73 (m, 6H). <sup>13</sup>C NMR (CDCl<sub>3</sub>, 125 MHz):  $\delta$  181.1, 163.0, 162.1, 160.2, 159.0, 143.7, 141.4, 132.1, 132.1, 132.1, 131.2, 131.1, 131.1, 131.0, 130.5, 130.4, 124.7, 124.7, 122.5, 122.4, 122.3, 121.8, 116.9, 115.5, 115.3, 111.7, 111.7, 111.5, 111.5, 104.4, 104.2, 104.0, 98.1, 79.1, 60.2, 47.5, 32.5, 30.5, 30.4, 21.4. HRMS: calcd for C<sub>28</sub>H<sub>26</sub>F<sub>3</sub>N<sub>2</sub>O<sub>5</sub> (M+H), 527.1794; found 527.1804.
- Overman, L. E.; Sugai, S. J. *Org. Chem.* **1985**, *50*, 4154.
- Molecular modeling and ligand docking on intasome: Molecular modeling of the crystal structure of prototype foamy virus (PFV) integrase intasome (PDB code 3OYA) with compounds **3** and **4** docked within the catalytic site was achieved by using the Surflex-Dock package within Sybyl-X [Sybyl-X 1.3 (winnt\_os5x) version] (Tripos, St. Louis, MO, 2011). Processing was done according to default conditions of Surflex-Dock and Biopolymer. The prepared ligands were docked to the intasome active site as guided by an appropriately generated protomol. The modeling was validated by screening a ligand set for compounds **3**, **4** and a number of known anti-HIV integrase inhibitors and all of the active compounds were recognized, including compounds **3** and **4**, and all showed significantly high total scores.
- Hare, S.; Gupta, S. S.; Valkov, E.; Engelman, A.; Cherepanov, P. *Nature* **2010**, *464*, 232.
- Bissantz, C.; Kuhn, B.; Stahl, M. J. *Med. Chem.* **2010**, *53*, 5061.
- Rademacher, P.; Khelashvili, L.; Kowski, K. *Org. Biomol. Chem.* **2005**, *3*, 2620.
- Steiner, T.; Koellner, G. J. *Mol. Biol.* **2001**, *305*, 535.
- Cytochrome P450: Structure, Mechanism, and Biochemistry*; Ortiz de Montellano, P. R., Ed.; 3rd ed.; Kluwer Academic/Plenum: New York, 2005.
- Baranczewski, P.; Stanczak, A.; Sundberg, K.; Svensson, R.; Wallin, A.; Jansson, J.; Garberg, P.; Postlind, H. *Pharmacol. Rep.* **2006**, *58*, 453.



19. Chauret, N.; Gauthier, A.; Martin, J.; Nicoll-Griffith, D. A. *Drug Metab. Dispos.* **1997**, *25*, 1130.
20. *Stability of compound 3 in pooled human liver microsomes*: Incubations contained 0.5 mg/mL protein, 50  $\mu$ M test compound, 2 mM NADPH, 0.5 U/mL G-6-P-DH, 5 mM  $\text{MgCl}_2$ , and 5 mM G-6-P in a final volume of 400  $\mu$ L in 100 mM potassium phosphate buffer (pH 7.4). The reaction mixture was pre-incubated for 3 min at 37 °C before initializing by addition of NADPH solution, followed by incubation for 60 min. A solution of 60  $\mu$ L was withdrawn at 0, 15, 30, 45 and 60 min and quenched with 60  $\mu$ L of ice-cold acetonitrile. The precipitated proteins were removed by centrifugation at 5000 $\times$ g for 5 min at room temperature before analysis of the supernatant by HPLC. Analysis was done using a reversed-phase HPLC column on a Beckman Coulter Gold 127 solvent system and Gold 166 UV analytical detector. The data were collected and processed using Gold software. The elution process involved: analytical column Delta Pak C18 (15  $\mu$ m, 300  $\times$  3.9 mm, 100 Å) with a mobile phase of (A) 10 mM potassium phosphate buffer (pH 6.5) and (B) acetonitrile, which were used as follows: 0–2 min, 20% B, 2–8 min, 20–80% B, 8–18 min, 80% B, 18–20 min, 20% B. The flow rate was kept at 1.5 mL/min, with UV detection at 360 nm. Retention times for compound **3** and its slowly produced metabolite were 10.48 and 9.1 min, respectively.
21. *Cytochrome P450 studies*: Incubation mixtures contained potassium phosphate buffer (100 mM, pH 7.4),  $\text{MgCl}_2$  (5 mM), the requisite substrate dissolved in an appropriate solvent, compound **3** (range of concentrations) and pooled human liver microsomes. The reaction mixture (final volume 100  $\mu$ L) was pre-incubated for 3 min at 37 °C before initiation of the reaction by the addition of NADPH (final concentration 2 mM). In each incubation mixture, the organic

solvent concentration was kept at or below 1.5% by volume. Each reaction was terminated by adding ice-cold acetonitrile (100  $\mu$ L). Proteins were precipitated from the samples by centrifugation at 5000 $\times$ g for 10 min at room temperature in a microcentrifuge tube. The supernatant was analyzed by HPLC-UV for detection of substrates and metabolites. Reversed-phase HPLC analyses were performed on a Beckman Coulter Gold 127 solvent system with a Gold 166 UV analytical detector. The data were collected and processed using a Gold software package. CYP HPLC analytical assays: Testosterone and 6 $\beta$ -hydroxytestosterone analysis involved analytical column Delta Pak C18 (15  $\mu$ m, 300  $\times$  3.9 mm, 100 Å) eluting with (A) 10 mM potassium phosphate buffer (pH 4.5) and (B) acetonitrile, in a gradient mixture starting with 25% (B) at time 0 min to 100% (B) at time 23 min, at a flow rate of 1.2 mL/min, with detection wavelength set at 254 nm. Testosterone and 6 $\beta$ -hydroxytestosterone were detected at 14.01 and 8.90 min rt, respectively. The analytical column Novapak C18 (4  $\mu$ m, 150  $\times$  3.9 mm, 60 Å) mounted on the above HPLC system was used in the analysis of triazolam and 4-hydroxytriazolam as well as dextromethorphan and dextrorphan respectively. The elution solvent for both assay system was similar to testosterone above with variation in gradient system. Triazolam and hydroxytriazolam were separated with a gradient solvent mixture of 30% (B) at 0 min to 100% B at 16 min, at a flow rate of 1.0 mL/min while detecting at 260 nm wavelength. The rt for Triazolam and hydroxytriazolam were 8.46 and 5.48 min, respectively. Dextromethorphan and dextrorphan were similarly separated with gradient solvent elution system of 28% (B) at 0 min to 100% (B) after 16 min, at a flow rate of 1.0 mL/min, with UV detection set at 278 nm. RT for dextromethorphan and dextrorphan were 11.96 and 5.96 min, respectively.